Material: Ferritic Steel: F82H
Property: Test Temperature (˚C) versus Normalized K (MPa*sqrt(m))
Condition: Unirradiated
Data: Experimental

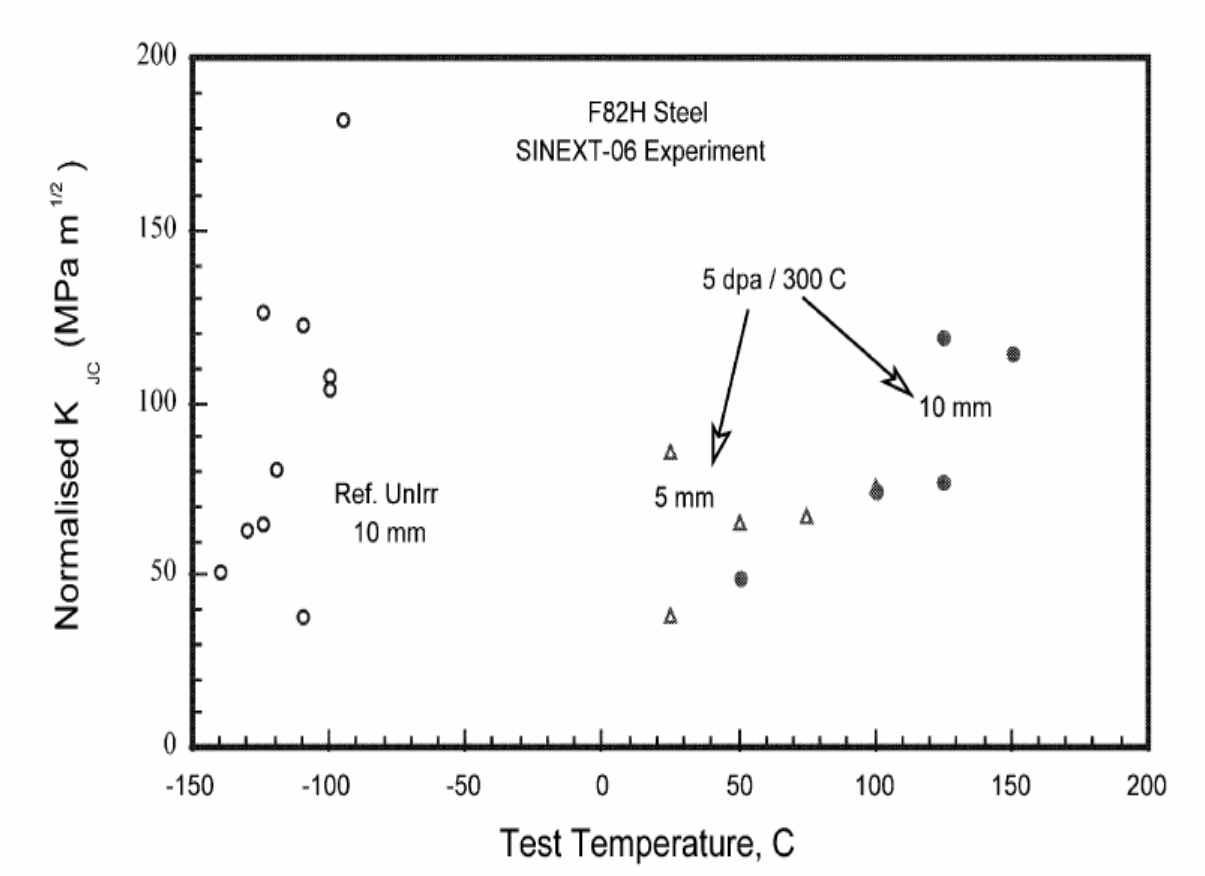

Source:
Fusion Engineering and Design, 61-62, (2002), 617-628

Title of paper (or report) this figure appeared in:
Materials Design Data for Reduced Activation Martensitic Steel type F82H

Author of paper or graph:
A.-A.F. Tavassoli, J.-W. Rensman, M. Schirra, K. Shiba

Caption:
25 mm normalized transition fracture toughness values for unirradiated and 300 ˚C irradiated specimens taken from a 5 mm F82H plate.
Note: All data is for F82H Steel SINEXT-06 Experiment.

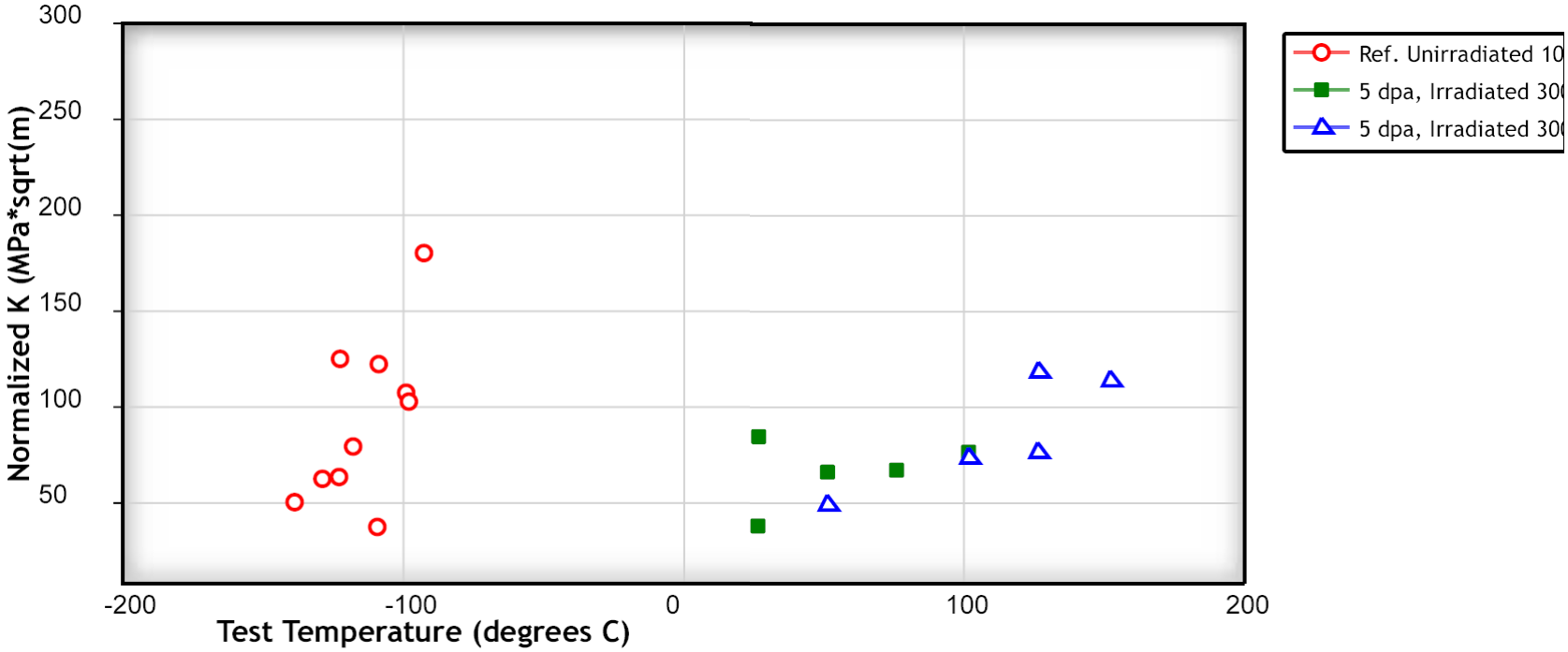

25 mm normalized transition fracture toughness values for unirradiated and 300 ˚C irradiated specimens taken from a 5 mm F82H plate. Note: All data is for F82H Steel SINEXT-06 Experiment.

Reference:

Author: *A.-A.F. Tavassoli, J.-W. Rensman, M. Schirra, K. Shiba*
Title: *Materials Design Data for Reduced Activation Martensitic Steel type F82H*
Source: *Fusion Engineering and Design, 2002, Volume 61-62, Page 617-628*, [PDF]

View Data | Author Comments

Plot Format:

Y-Scale: ◉ linear ○ log ○ ln
X-Scale: ◉ linear ○ log ○ ln

Update | Close Window

ELSEVIER

Fusion Engineering and Design 61–62 (2002) 617–628

Fusion Engineering and Design

www.elsevier.com/locate/fusengdes

Materials design data for reduced activation martensitic steel type F82H

A.-A.F. Tavassoli [a,*], J.-W. Rensman [b], M. Schirra [c], K. Shiba [d]

[a] *DMN/Dir, Commissariat à l'Energie Atomique, CEA/Saclay, 91191 Gif sur Yvette Cedex, France*
[b] *NRG, Petten, The Netherlands*
[c] *FZK, Germany*
[d] *JAERI, Japan*

Abstract

This paper presents materials data for design of ITER test blanket modules with the reduced activation ferritic martensitic steel type F82H as structural material. From the physical properties databases, variations of modulus of elasticity, density, thermal conductivity, thermal diffusivity, specific heat, mean and instantaneous linear coefficients of thermal expansion versus temperature are derived. Also reported are Poisson's ratio and magnetic properties. From the tension test results, nominal and minimum stress values of S_y and S_u are derived and used for calculation of allowable primary membrane stress intensity S_m. Likewise, uniform and total elongations, as well as reduction of area data, are used for calculation of minimum and true ductility at rupture values. From the instrumented Charpy impact and fracture toughness test data, ductile to brittle transition temperature, toughness and behavior of material in different fracture modes are evaluated. The effect of specimen size and geometry are discussed but preference is given to standard size specimens. From the fatigue data, total strain range versus number of cycles to failure curves are plotted and used to derive fatigue design curves, using a reduction factor of 2 on strain and a reduction factor of 20 on number of cycles to failure. Cyclic hardening curves are also derived and compared with monotonic hardening curves. From the creep data, time dependent allowable stresses S_r and S_t are calculated. Combination of tension and creep results are used to deduce S_{mt} and isochronus curves. Finally, irradiated and aged materials data are compared to insure that the safety margins incorporated in unirradiated design limits are not exceeded.

Keywords: Ferritic martensitic steel; Materials data; ITER test blanket modules

1. Introduction

ITER detailed design report [1] is supported by an interim structural design criteria (IISDC) [2] where materials physical and mechanical properties are presented in a document similar to that of the 'Appendix A: Materials data and Analysis' in the RCC-MR [3]. However, ITER documents are written mainly for austenitic stainless steels [4,5] and deal with low temperatures and low neutron doses. They do not include at present rules and data for reduced activation ferritic/martensitic

* Corresponding author. Tel.: +33-1-6908-6021; fax: +33-6908-8070
E-mail address: tavassoli@cea.fr (A.-A.F. Tavassoli).

0920-3796/02/$ - see front matter
PII: S0920-3796(02)00255-7

steels (RAFM steels), the primary structural material considered for ITER test blanket modules and a DEMOnstration reactor. While the time-schedule for development of demo interim structural design criteria (DISDC) is relatively long, that of the ITBM is short and concurrent with ITER.

The two prominent blanket module concepts to be tested in ITER are water cooled lithium lead (WCLL) and helium cooled pebble bed (HCPB) [6]. Both of these modules use RAFM steel as structural material. This is also the case for a third type of blanket module being investigated (lithium–lead self-cooled module). The basic material data requirements for all these concepts are similar. Of course the differences in service temperature, cooling media, fabrication procedures, coating, He/dpa ratio, etc. have to be incorporated in the final design data calculation.

RAFM steels are alloys whose main compositions are derived from the conventional modified 9Cr–1Mo steel [7], but with the high activation elements, such as Mo and Nb, replaced by their equivalent low activation elements (e.g. W, V and Ta). The presence of high activation residual elements is kept as low as possible.

Presently the only RAFM steel with sufficient data for code analysis is the steel produced in Japan (F82H) [8] and tested under the IEA fusion materials collaborative agreement. Materials properties data of this steel are used in this paper. Experimental data on the European RAFM steel, Eurofer [9], are not yet adequate.

2. Procedures

Appendix A begins with the section A.GEN [2], which contains the definitions of the physical and mechanical properties used in the ISDC together with the formulae used in calculating the various design limits. Subsequent sections of Appendix A contain design data for materials, each section being identified by a letter and a number (e.g, S: structural material, S1: type 316 L(N)-IG stainless steel, S18: Mod. 9Cr1Mo (Z10 CDVNB 9.1), B: bolting, etc.). In this paper, individual nuances of S18 are identified by an additional letter, e.g. S18F for F82H and S18E for Eurofer.

When writing the Appendix A for RAFM steels, a particular attention is paid to the quality of data. All materials properties data collected and used are fully traceable and are obtained and analysed according to an internationally accepted procedure [10]. Data obtained from tests on small or non-standard specimens are only used for comparison or substantiation of data from tests on standard specimens.

3. Results

Section and sub-section numbering used here below are without A3.S18F that precedes these in the Appendix A procedures of DISDC. To save space many tables and figures are also omitted. For full description of results refer to the actual Appendix A report [11].

4. Introduction and products

4.1. Introduction

Most of the data used in the A3.S18F are from the two 5000 kg heats (9741, 9753) produced by NKK/Japan [8] and tested by the IEA partners under an implementing agreement on the fusion materials [10].

4.2. Products and compositions

F82H is a fully martensitic steel (Fe–8Cr–2W) with small additions of C, Si, Mn, Ti, V and Ta. The content of all impurities and in particular the high activation elements are kept low.

Plates from the heat 9741 are supplied in 7.5 and 15 mm thickness and from heat 9753 in 15 and 25 mm plates. All plates are normalized at 1040 °C for 37–40 mn (according to thickness) and tempered at 750 °C for 60 mn [8].

Hardness of the as received material is 215–219 (HV 10).

4.3. Quality safe guarding data

Tentative recommendations are similar to those specified for conventional 9Cr–1Mo steel [3,7].

5. Physical properties

5.1. Coefficients of linear thermal expansion

Variation of mean linear coefficient of thermal expansion (α_m) up to 800 °C can be described through a simple equation. At above 800 °C, however, there is a sharp drop in α_m and the equation is not valid beyond.

$$\alpha_m = 9.0955 + 4.6477\times10^{-3}\,(\theta+273) - 1.2141\times10^{-6}\,(\theta+273)^2$$

where α is in 10^{-6}/K and θ in °C. At room temperature the value of α_m is 10.7×10^{-6}/K.

5.2. Elastic and rigidity moduli

Variations of elastic (E) and rigidity (G) moduli versus temperature ($20<\theta<700$ °C) are given by:

$$E = 218.76 - 0.077834\theta + 1.4735\times10^{-4}\theta^2 - 2.1998\times10^{-7}\theta^3$$

$$G = 84.902 - 0.03378\theta + 6.8965\times10^{-5}\theta^2 - 9.828\times10^{-8}\theta^3$$

where E and G are in GPa, θ in °C. At room temperature the values obtained are: $G=84$ GPa, $E=217$ GPa.

5.3. Poisson's ratio

Poisson's ratio varies from 0.29 to 0.31 and has an average value of 0.3.

5.4. Density

Only room temperature value ($\rho_{(RT)}=7871$ kg/m^3) is available but rough extrapolation to higher temperatures can be made using the trend from conventional 9Cr–1Mo steel.

5.5. Specific heat, thermal conductivity, thermal diffusivity

The equations describing variations of the specific heat (C_p), thermal conductivity (k), and thermal diffusivity (a) as a function of test temperature are given below (validity up to about 870 °C):

$$C_p = 1390.2 - 7.8498(\theta+273) + 0.022969(\theta+273)^2 - 2.7446\times10^{-5}(\theta+273)^3 + 1.1932\times10^{-8}(\theta+273)^4$$

$$k = 28.384 - 0.011777(\theta+273) - 1.0632\times10^{-6}(\theta+273)^2 - 8.2935\times10^{-9}(\theta+273)^3$$

$$a = 0.089188 + 1.4051\times10^{-5}(\theta+273) - 5.7859\times10^{-8}(\theta+273)^2$$

Values at room temperature are: $C_p=448$ J/kg K, $k=31.3$ W/m K, $a=0.0885\times10^{-6}$ m^2/s and θ is in °C.

5.6. Electrical resistivity

As an interim step values of conventional 9Cr–1Mo steel are used. They are for instance: 0.502×10^{-6} at RT, 0.722×10^{-6} at 300 °C and 0.886×10^{-6} at 500 ohm.m.

5.7. Magnetic properties

Magnetic properties of F82H are summarized in Table 1.

Table 1
Summary of F82H steel magnetic properties (source JAERI [8])

T (K)	File	Mass (kg)	σ (EMU/g)	H_{max} (Oe)	B_s (Gauss)	B_r (Gauss)	S_q	S^* (A/H_c)	H_c (Oe)	ΔH (Oe)	Std (dH/H_c)
300	RTL	0.161	1.983×10^2	1.500×10^2	1.967×10^4	2.162×10^2	1.100×10^{-2}	4.496×10^{-2}	1.462×10	2.264×10^3	1.549×10^2
	RTC	0.170	1.960×10^2	1.500×10^2	1.943×10^4	2.009×10^2	1.034×10^{-2}	1.659×10^{-2}	1.473×10	2.549×10^3	1.731×10^2
473	200L	0.161	1.910×10^2	1.500×10^2	1.894×10^4	2.080×10^2	1.098×10^{-2}	4.067×10^{-2}	1.372×10	2.235×10^3	1.629×10^2
	200C1	0.170	1.881×10^2	1.500×10^2	1.866×10^4	1.931×10^2	1.035×10^{-2}	2.941×10^{-2}	1.417×10	2.452×10^3	1.731×10^2
573	300L	0.161	1.848×10^2	1.500×10^2	1.833×10^4	1.895×10^2	1.034×10^{-2}	1.672×10^{-2}	1.278×10	2.160×10^3	1.691×10^2
	300C	0.170	1.822×10^2	1.500×10^2	1.807×10^4	1.697×10^2	9.388×10^{-3}	3.333×10^{-2}	1.250×10	2.367×10^3	1.893×10^2
673	400L	0.161	1.765×10^2	1.500×10^2	1.750×10^4	1.668×10^2	9.533×10^{-3}	6.216×10^{-2}	1.115×10	2.060×10^3	1.847×10^2
	400C	0.170	1.740×10^2	1.500×10^2	1.726×10^4	1.697×10^2	9.830×10^{-3}	-1.214×10^{-2}	1.214×10	2.233×10^3	1.839×10^2

6. Tensile strength properties

6.1. Minimum and average yield strength at 0.2% offset

A third degree polynomial equation is fitted to all S_y data disregarding the specimen orientation. The minimum curve is derived from this fit (−1.96 standard deviation at RT). Equations describing both average and minimum curves are given below and values at temperatures 20–700 °C in Table 2. Stress values are in MPa and temperature in °C.

$$S_{y(av)} = 558.76 - 0.81574\theta + 2.7621\times10^{-3}\theta^2 - 3.476 \times 10^{-6}\theta^3$$

$$S_{y(min)} = 0.9025(558.76 - 0.81574\theta + 2.7621\times10^{-3}\theta^2 - 3.476\times10^{-6}\theta^3)$$

6.2. Minimum and average ultimate tensile strength

Similar procedures are used for S_u (Table 3)

$$S_{u(av)} = 666.44 - 0.84514\theta + 2.1019\times10^{-3}\theta^2 - 2.617 \times 10^{-6}\theta^3$$

$$S_{u(min)} = 0.9384(666.44 - 0.84514\theta + 2.1019\times10^{-3}\theta^2 - 2.617 \times 10^{-6}\theta^3)$$

Notice that

a) The effect of prolonged aging at service temperature is bound by minimum curves.
b) Weld data show a large scatter but are also mostly bound by the minimum curves.
c) Irradiation hardening is observed at very low doses when the temperature is less than 350 °C. Equation describing the variations of S_y as a function of irradiation dose (dpa) for temperatures 300–325 °C is given by:

$$S_{y(irr)} = S_{y(av,unirr)}(1 + 0.56628\phi + 0.44327\phi^{1.0673})$$

More recent data (up to 12 dpa) confirm the above trend and show that yield strength of base and weld materials converge and saturate at doses

Table 2
Minimum and average yield stress values

Temp. (°C)	20	100	200	250	300	350	400	450	500	550	600	650	700
$S_{y(av)}$ (MPa) plate	544	501	478	473	469	463	452	434	407	367	313	241	149
$S_{y(min)}$ (MPa) plate	491	452	432	427	423	417	408	392	367	332	282	217	134

Table 3
Minimum and average ultimate tensile strength values

Temp. (°C)	20	100	200	250	300	350	400	450	500	550	600	650	700
$S_{u(av)}$ (MPa) plate	650	600	561	546	531	516	497	473	442	402	351	286	207
$S_{u(min)}$ (MPa) plate	610	563	526	512	499	484	467	444	415	377	329	269	194

higher than 5 dpa ($S_{y(irr)} = 850$ MPa at 300 °C) [12]. S_u also increases with increasing irradiation dose but at a lower rate.

6.3. Minimum uniform elongation

These values are derived from the plots of uniform elongation versus test temperature.

The minimum uniform elongation drops below 0.5% at doses >2 dpa. For doses less than 2 dpa, $\varepsilon_{u(min)} = 0.5\%$.

6.4. Minimum true strain at rupture

Minimum true strain at rupture is calculated from

$$\varepsilon_{tr} = \ln\left(\frac{100}{100 - \%RA}\right)$$

where %RA is reduction of area at rupture from tension test, in the unirradiated condition it is $>$ 70%.

$\varepsilon_{tr} = 1.0\%$

6.5. Minimum stress to rupture

Average and minimum equations describing evolution of the creep rupture stress versus the Larson–Miller parameter P for test temperatures up to 600 °C are:

$$\sigma_{av} = 3708.8 - 360.42P + 13.359P^2 - 0.18482P^3$$

$$\sigma_{min} = 3708.8 - 360.42P + 13.359P^2 - 0.18482P^3 - 1.96 \times 10.39$$

where $P = (26 + \log t) \times (\theta + 273)/1000$ and 10.39 is standard deviation.

Notice: F82H oxidizes at high temperatures and therefore high temperature creep tests are performed in vacuum, Fig. 2.

6.6. Minimum creep ductility

Minimum observed creep elongation at rupture for tests performed at 450–700°C is greater than 5%, hence $\varepsilon_c = 5\%$.

6.7. Minimum true strain at rupture for creep

Minimum true creep strain at rupture is obtained from the reduction of area of at rupture of creep specimens in a similar manner as that explained for tensile elongation, it is tentatively assumed $\varepsilon_{ctr} = 1\%$.

7. Curves for tests on creep and swelling

7.1. Negligible thermal creep curve

At temperatures less than about 425 °C thermal creep of conventional modified 9Cr steel is

ignored. The behavior of F82H is similar. At 550 °C, the time to reach 0.05% strain under a stress of 189 MPa ($=1.5S_m$), is less than about 2 h.

7.2. Swelling curve (ϕt_{s1}) for the test to determine if nonlinear analysis is needed

Swelling is ignored for RAFM steels at low doses. These steels are well known for their excellent resistance to swelling at high doses.

7.3. Negligible swelling curve

Also ignored for RAFM steels at ITBM doses.

7.4. Irradiation induced creep curve (ϕt_{c1}) for the test to determine if nonlinear analysis is needed

The fluence (ϕt_{c1}) for test to determine if nonlinear analysis is needed, is defined by the fluence to accumulate a creep strain of 2% at a stress of S_m (T, ϕt). It is ignored at ITBM doses.

7.5. Negligible irradiation induced creep curve

The fluence for negligible irradiation-induced creep is defined by the fluence to accumulate a creep strain of 0.05% at a stress of $1.5S_m$ (T, ϕt). This property requires additional analysis.

8. Analysis data

8.1. Values of S_m

S_m in RAFM steels is governed by S_u (see Fig. 1). The equation describing the evolution of S_m versus temperatures is given below and values obtained in Table 4.

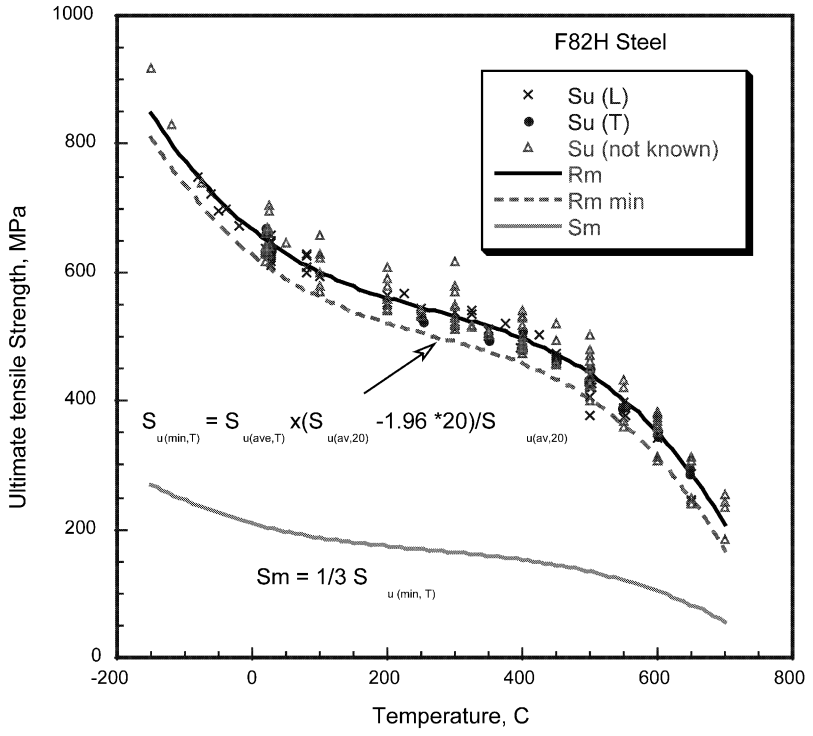

Fig. 1. Plot of S_u data vs. temperature, with average, minimum S_m curves.

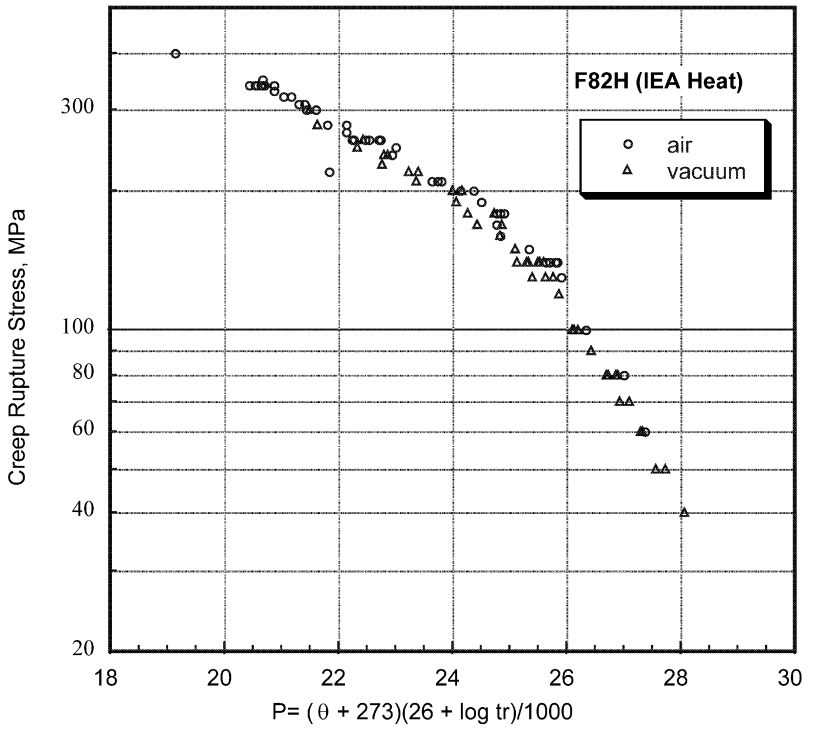

Fig. 2. Evolution of creep–rupture stress versus Larson–Miller parameter (high temperature tests are performed in vacuum).

$$S_m = 0.3128(666.44 - 0.84514\theta + 2.1019\times10^{-3}\theta^2 - 2.617\times10^{-6}\theta^3)$$

8.2. Values of S_t

Maximum allowable creep stress values (S_t) at a given temperature for a given time are derived from 2/3 of minimum stress to rupture and are reported in Table 5. S_{mt} (combination of S_m and S_t) is governed by S_m for ITBM service conditions and only at temperatures about 525 °C and above, S_t becomes lower than S_m for times considered here.

8.3. Values of S_r

Minimum stress rupture values, S_r, are derived from stress rupture data, see Section 6.5.

8.4. Fatigue curves at saturation

See Section 9.4.

8.5. Isochronus and creep deformation curves

Isochronus curves are obtained from adding tensile ($\varepsilon_e+\varepsilon_p$) and creep ($\varepsilon_c$) strains:

$$\varepsilon_t = \varepsilon_e + \varepsilon_p + \varepsilon_c$$

The average curves obtained are shown in Fig. 3.

8.6. Values of S_{Rh} and S_{Rc}

Stress relaxation behavior of F82H steel is not known, that of Mod. 9Cr1Mo is used as an interim step.

8.7. Symetrization factor, K_s

Not available for F82H steel and should be very sensitive to strain as is for Mod. 9Cr1Mo.

Table 4
S_m values versus temperature

Temp. (°C)	20	100	200	250	300	350	400	450	500	550	600	650	700
S_m (MPa)	204	188	176	171	166	162	156	148	139	126	110	90	65

Table 5
Values of S_t at temperatures 425–675 °C

Time (h)	425 °C	450 °C	475 °C	500 °C	525 °C	550 °C	575 °C	600 °C	625 °C	650 °C	675 °C
10	303	276	252	229	207	186	166	146	127	107	87
30	289	264	239	217	195	174	154	134	114	94	73
100	276	250	226	204	182	161	141	121	100	80	58
300	263	238	215	192	171	150	129	109	88	66	44
1000	250	226	202	180	159	137	117	95	74	51	27
3000	239	214	191	169	147	126	105	83	60	37	12
10 000	226	202	179	157	135	114	92	69	45	21	
30 000	216	192	169	146	124	102	80	56	31	5	
100 000	204	180	157	135	112	89	66	41	15		
300 000	194	170	147	124	101	78	53	28			

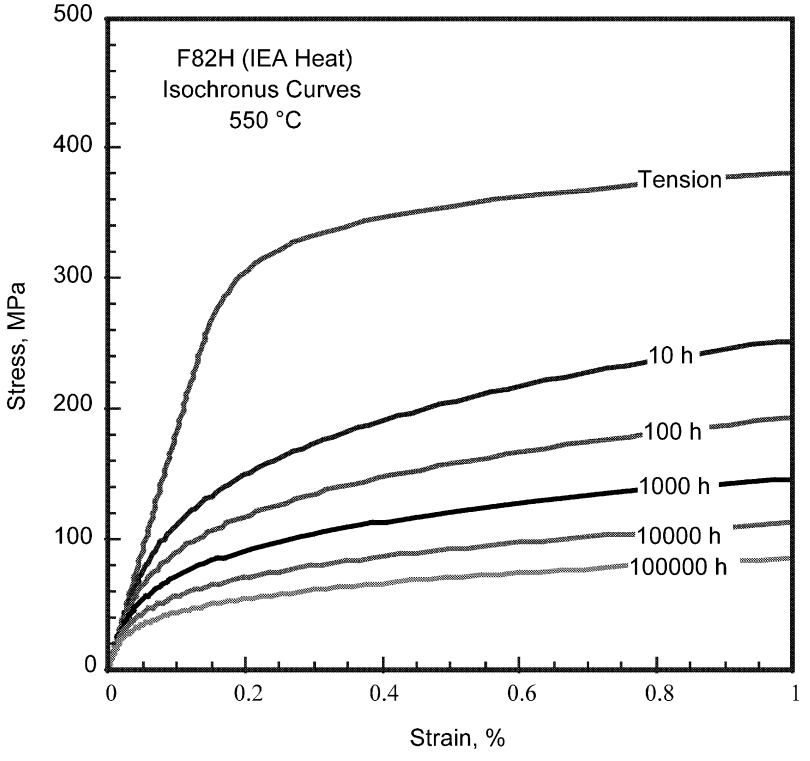

Fig. 3. Isochronous curves of F82H steel at 550 °C.

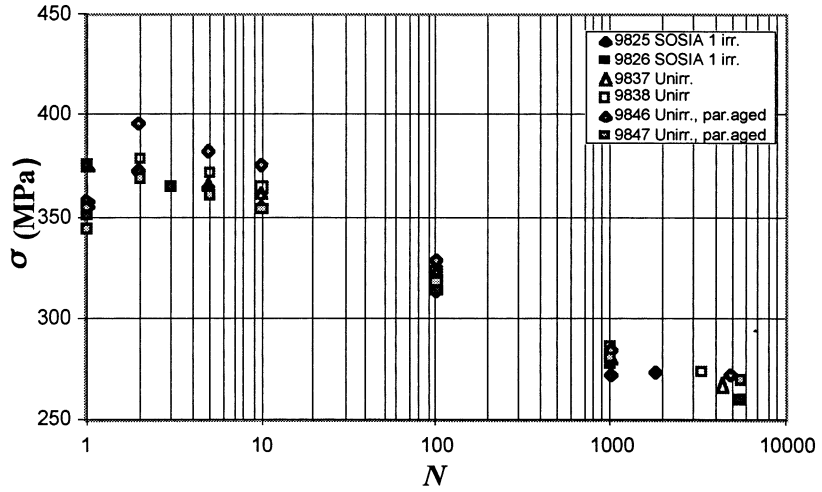

Fig. 4. Evolution of the peak stress in tension during fatigue of F82H (7.5 mm reference plate tested at 500 °C, $\Delta\varepsilon_t = 0.6\%$, monitors aged at test temperature) [13].

8.8. Creep–fatigue interaction diagram

Experimental data are still being collected.

Calculation of creep–fatigue damage in RAFM steels is complicated because of continuous variation of stress throughout the fatigue life.

8.9. Cyclic curves, values of K_ε and K_v

As shown in Fig. 4, F82H steel shows cyclic softening rather than cyclic hardening. For conventional analysis the total strain at half fatigue life is used:

$$\varepsilon_t = 100\sigma/E + (\sigma/K)^{1/m}$$

Tentative values of K and m are calculated and reported in Table 6 using only data reported for parallel sided standard specimens.

9. Additional analyses

9.1. Monotonic hardening curve in tension

Average monotonic hardening curves in tension are deduced from the sum of elastic and plastic strains.

$$\varepsilon_t = \varepsilon_e + \varepsilon_p$$

$$\varepsilon_t = 100S_{y(av)}/E + (S_{y(av)}/CS_y)^{1/n}$$

Values of C and n are obtained from log–log plots of normalized stress $S_y/S_{y(av)}$ at test temperature versus plastic strain. Minimum hardening curves are obtained by replacing $S_{y(av)}$ with $S_{y(min)}$.

Notice: for a better comparison with cyclic hardening curves often values taken from the first fatigue cycle are used.

9.2. Bilinear curves

Not calculated.

9.3. Creep deformation curve

Creep deformation curves are obtained by combining primary (ε_{epc}) and secondary creep ($\varepsilon_s = C\sigma^n t$).

Primary creep at temperatures less than 425 °C is ignored.

$$\varepsilon_c = 0 \quad \text{if} \quad \theta \leq 425\ ^\circ\text{C}$$

At higher temperatures it is expressed by:

$$\varepsilon_c = C_1 t^{C2}\sigma^{C3} \quad 425 < \theta < 700\ ^\circ\text{C}$$

with an upper limit of time (t_{epc}) and strain (ε_{epc}) taken from the end of primary creep. The creep

Table 6
Values of K and m for cyclic hardening curves

θ (°C)	K	m
20	502	0.08874
300	371	0.13023
550	337	0.06206

strain from secondary creep is then added.

$$\varepsilon_s' = C\sigma^n$$

and used in the creep deformation equation:

$$\varepsilon_c = \varepsilon_{epc} + 100C\sigma^n(t - t_{epc})$$

Coefficients, constants and exponents of the above equations are deduced from fits to the experimental data.

9.4. Fatigue curves

Fig. 5 shows available fatigue data in terms of total strain range $\Delta\varepsilon_t$ versus number of cycles to rupture N_r. More recently irradiated fatigue data have become available but the scatter in results (combination of HIP and wrought results and diametral extensometry) hinders their full exploitation at this stage [13]. Tentative design values are deducted from a smooth curve fitted to the minimum of curves obtained from $\Delta\varepsilon_t/2$ and $N_f/20$ of the average curve fitted to an average curve (20–550 °C) of axial extensometry results (Table 7).

9.5. Maximum allowable damage

$$D_{max} = 1\%$$

9.6. Fracture toughness

The ductile to brittle transition temperature of F82H steel in the as received conditions is usually less than −50 °C. Small differences are observed between results of standard size specimens (10 × 10 × 55 mm in both LT and TL orientations) and mini-CV specimens (2.5 × 10 × 55 mm^3 in LT orientation) or KLST specimens (3 × 4 × 4 mm).

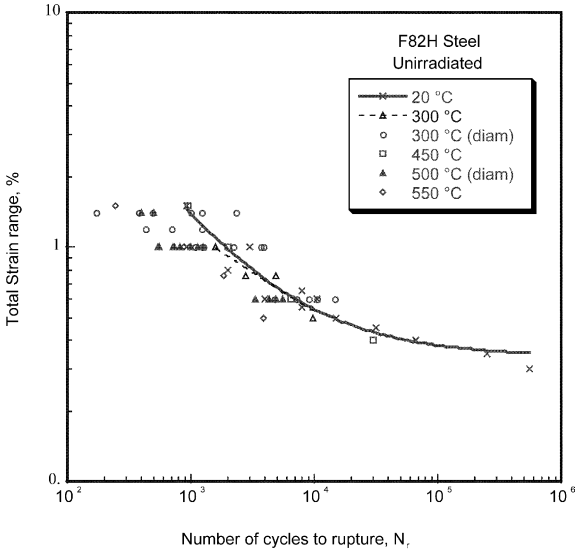

Fig. 5. Continuous fatigue data of F82H steel, all tests in fully reversible strain controlled mode (notice large scatter in results with diametral extensometry).

In general, smaller specimens show more optimistic results.

Equation fitted to mini-CV data is:

$$K_{cv} = 134.16 + 134.16\exp((\theta - 63.685)/24.999)$$

Here K_{CV} is in J/cm^2 and θ in °C. Ageing at temperatures higher than 550 °C, and in particular irradiation at temperatures less than about 350 °C, shift the DBTT to higher temperatures.

The quasi-static fracture toughness of 5 and 10 mm thick compact tension specimens taken from 25 mm plates of F82H steel and normalized to 25 mm thickness specimens (Fig. 6) show a higher shift in DBTT. The shift in T_o is from −110 to 125 °C, i.e. 235 °C, after 5 dpa [12].

10. Conclusions

Materials design data situation for the F82H steel is adequately advanced to allow reliable preliminary design analysis for ITBM. In some cases such as fatigue and creep–fatigue, additional experimental data are needed.

Table 7
Coefficients A and B in the Langer equation from fit to unirradiated data (20–550 °C)

Temp. (°C)	A	B	$\Delta\varepsilon_0$	Validity, $\Delta\varepsilon_t$ (%)
20 °C	16.11	−0.3918	0.094	< 2.0
Average	48.08	−0.58329	0.31347	< 2.0
Design	7.4873	0.51083	0.17379	< 2.0

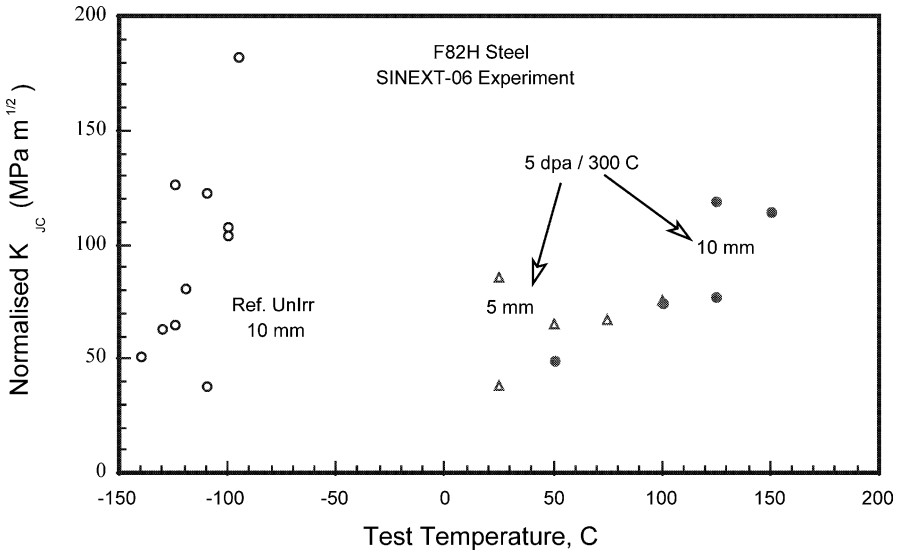

Fig. 6. 25 mm normalized transition fracture toughness values for unirradiated and 300 °C irradiated specimens taken from a 5 mm F82H plate [12].

Acknowledgements

The results used in this work come from the European RAFM database that is still expanding. Several European, American, Russian and Japanese institutes have contributed to this database. The main contributing institutes and principal investigators are: from Europe: CEA (A. Alamo, E. Rigal, L. Bedel, J.-M. Gentzbittel), CIEMAT (P. Fernãndez, A.-M. Lancha, J. Lapeña), CRPP (N. Baluc, P. Spätig, M. Victoria), ENEA (G. Filacchioni, C. Fazio), FZK (E. Diegele, K. Ehrlich, R. Lindau, A. Möslang, K. Petersen, Schaefer, M. Schirra, R. Schmitt), NRG (B. van der Schaaf, J.-W. Rensman), NFR (S. Tähtinen), RISOE (B.N. Singh), SCK (E. Lucon), VTT (A. Lind); from Japan: NKK, JAERI (K. Shiba, S. Jitsukawa) and Universities of Kyoto (A. Kohyama), Tohuko (H. Matsui) and Tokyo (K. Abe); from the USA: ORNL (R. Klueh, J.-P. Robertson, S. Zinkle), ANL (S. Majumdar), PNNL (D. Gelles) and the Universities of Illinois (J.F. Stubbins) and California at Santa Barbara (G.R. Odette, G.E. Lucas). They wish also to express their gratitude to the European Union (S. Païdassi) and EFDA-CSU (M. Gasparotto, G. Le Marois) for their financial and technical support.

References

[1] ITER detailed design report, ITER JCT, Garching JWS, Germany, 2001.
[2] P. Smith (Ed.), ITER interim structural design criteria (IISDC), Draft 5, doc. no. S74 RE 2 96-06-18 W 1.1, ITER, ITER JCT, 1996.

[3] RCC-MR 'Règles de Conception et de Construction des Matériels Mécaniques des îlots nucléaires RNR.', Tomes, I et II, AFCEN, édition 1993.
[4] A.-A. Tavassoli, Fusion Eng. Des. 29 (1995) 371–390.
[5] A.A. Tavassoli, F. Touboul, J. Nucl. Mater. 233–237 (1996) 51–61.
[6] A.R. Raffray, M. Akia, V. Chuyanov, L. Giancarli, S. Malang, Breeding blanket concepts for fusion and materials requirements, in 10th International Conference on Fusion Reactor Materials, Baden-Baden, Germany, 14–19 October, 2001.
[7] J. Waering, A.A. Tavassoli, Assessment of martensitic steels for advanced fusion reactors, in: S.V. Möller, J.D. Riera (Eds.), Transactions of the 13th International Conference on Structural Mechanics In Reactor Technology, Porto Alegre, Brazil, 13–18 August, 1995, Division E, 563-574, Universidade Federal do Rio Grande du Sul (UFRGS).
[8] K. Shiba, Report of JAERI-Tech-97-038, JAERI, Tokyo, Japan, 1998.
[9] R. Lindau, M. Schirra, Fusion Eng. Des. 58–59 (2001) 781.
[10] S. Jitsukawa, M. Tamura, B. van der Schaaf, R.L. Klueh, A. Alamo, C. Peterson, M. Schirra, G.R. Odette, A.A. Tavassoli, K. Shiba, A. Kohyama, A. Kimura, Development and the database of a reduced activation martensitic steel F82H for fusion reactors, in 10th International Conference on Fusion Reactor Materials, Baden-Baden, Germany, 14–19 October, 2001.
[11] A.A. Tavassoli, RAFM Steels—Rules for design and inspection, Annual report of the Association Euratom/CEA 2000, 235-237, with full Appendix A text available from EFDA, Garching, Germany.
[12] J. Rensman, J. van Hoepen, J.B.M. Bakker, R. den Boef, F.P. van den Broek, E.D.L. van Essen, Tensile properties and transition behaviour of RAFM steel plate and welds irradiated up to 10 dpa at 300 °C, in 10th International Conference on Fusion Reactor Materials, Baden-Baden, Germany, 14–19 October, 2001.
[13] J.A. Vreeling, J. van Hoepen, J. Boskeljon, J. Rensman, Low cycle fatigue tests on F82H plate and powder HIP material, unirradiated and 300 and 500 °C neutron irradiated materials, NRG report 45714, Petten, The Netherlands, January, 2002.